

Silicon Temperature Measurement by Infrared Absorption: Fundamental Processes and Doping Effects

James C. Sturm, *Member, IEEE*, and Casper M. Reaves, *Student Member, IEEE*

Abstract—The temperature of silicon wafers may be inferred by measuring the transmission of infrared light through the wafers. In this paper, the fundamental absorption mechanisms in silicon at 1.30 and 1.55 μm have been investigated in the temperature range of 500–800°C. For lightly doped wafers in this temperature range, the absorption at 1.55 μm is by free carriers, and that at 1.30 μm is predominantly by bandgap absorption. The effect of heavy substrate doping on infrared absorption at elevated temperature has also been studied, and it was found that doping has little effect below levels of $7 \times 10^{17} \text{ cm}^{-3}$. Above that level the temperature dependence of free carrier absorption strongly affects the transmission as a function of temperature. The knowledge of the fundamental absorption processes is then used to predict the ultimate temperature ranges over which the technique will be useful.

I. INTRODUCTION

TEMPERATURE measurement has long been an issue in the rapid thermal processing field. The problem is especially severe at low temperature ($\leq 800^\circ\text{C}$) because of the long wavelengths necessary for pyrometry, the dependence of emissivity on wafer temperature [1], doping, and surface finish [2], and because of interference from the lamp spectrum. One attractive technique for measuring silicon wafer temperature in the 500–800°C range is the *in situ* measurement of the infrared absorption of the silicon wafer [3]. Because of the strong temperature dependence of silicon optical absorption in the 1.30- to 1.55- μm range, this method makes it possible to measure the wafer temperature with an accuracy on the order of 1°C. The method can be used for the growth of homoepitaxial and heteroepitaxial ($\text{Si}_{1-x}\text{Ge}_x$) [4] layers on the silicon substrates.

In this paper, the fundamental optical absorption processes in silicon in the 1.3- to 1.55- μm range are studied and identified, and the knowledge of these processes is

used to predict the range of application of the infrared transmission technique for measuring the temperature of silicon wafers. The absorption processes are also studied as a function of the doping level, and the effects of high wafer doping on this temperature measurement method are documented.

II. TEMPERATURE MEASUREMENTS BY INFRARED TRANSMISSION

The experimental apparatus for the measurement of infrared transmission in a rapid thermal chemical vapor deposition apparatus is shown in Fig. 1. Semiconductor lasers at 1.30 and 1.55 μm are modulated at different frequencies and coupled onto a common fiber. The uncertainty in the wavelengths is $\pm 0.01 \mu\text{m}$. The light is then projected onto the substrate. The beam size on the wafer is $\sim 1 \text{ cm}^2$, and the optical power is $\sim 1 \text{ mW}$. This low power density insures a noninvasive technique. A photodiode operated in short-circuit current mode and amplifier generate the detected signal, and lock-in amplifiers are used to recover the transmitted signals independent of any interference from the lamps.

The signal detected by the lock-in amplifier (denoted by $s(T)$) is a function of the temperature of the substrate. Assuming a uniform substrate and two perfectly parallel flat wafer surfaces, one can express $s(T)$ as

$$s(T) = \frac{K(1 - R(T))^2 \cdot e^{-\alpha(T) \cdot d}}{1 - (R(T))^2 \cdot e^{-2\alpha(T) \cdot d}} \quad (1)$$

where $R(T)$ is the power reflection coefficient at the silicon surface at temperature T , $\alpha(T)$ is the absorption coefficient at the relevant wavelength at temperature T , d is the wafer thickness, and K is a constant which depends on the laser power, detector efficiency, optical alignment, scattering from the rough wafer backside, etc. Interference effects (i.e., Fabry-Perot resonance) from phase coherence of multiple reflections within the wafer have been neglected due to the extremely short coherence length of the semiconductor lasers, and because of the rough wafer backside. The term in the denominator of (1) arises from multiple internal reflections within the wafer. Given a silicon reflectivity R of $\sim 30\%$, this denominator would dif-

Manuscript received February 28, 1991; revised August 2, 1991. This work was supported by ONR, under Contract N00014-90-J-1316, NSF, Texas Instruments, the New Jersey Commission on Science and Technology, IBM (furnace donations), and SRC.

J. C. Sturm is with the Department of Electrical Engineering, Princeton University, Princeton, NJ 08544.

C. M. Reaves was with the Department of Electrical Engineering, Princeton University, Princeton, NJ 08544. He is now with the University of California at Santa Barbara, Santa Barbara, CA 93106.

IEEE Log Number 9104306.

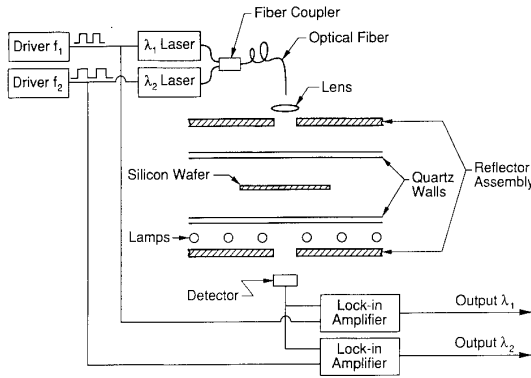


Fig. 1. Schematic cross section of the rapid thermal chemical vapor deposition apparatus modified for *in situ* measurement of infrared transmission.

fer at most by 9% from 1.00. Further, the rough wafer backside causes scattering which reduces the detected signal by at least a factor of 10 over that which would be received with a smooth surface. Since multiple reflected signals will scatter many times from this rough surface, multiple internal reflection can be ignored in this problem, with the resulting error less than 1%.

The detected signal is then

$$s(T) = K(1 - R(T))^2 \cdot e^{-\alpha(T)d}. \quad (2)$$

To eliminate the factor K (which contains many unknowns such as the laser power and backside roughness), the transmitted signal for all wafers is normalized (divided) by its cold value $s(NT)$. NT indicates the normalization temperature which is typically near room temperature. Such a normalization technique has previously been used by Jellison and Lowndes [5]. This normalized transmission $t(T)$ is then

$$t(T) = \frac{(1 - R(T))^2 \cdot e^{-\alpha(T)d}}{(1 - R(NT))^2 \cdot e^{-\alpha(NT)d}}. \quad (3)$$

A further simplification can be made by realizing that silicon reflectivity in the 1.3- to 1.5- μm range is only a very weak function of temperature. Based on the data of Lukes [6], the power transmitted of an air-silicon interface ($1 - R$) is expected to change by less than 2% from room temperature to 700°C. Therefore, with little error $t(T)$ reduces to

$$t(T) = e^{-\{\alpha(T) - \alpha(NT)\} \cdot d}. \quad (4)$$

From this simple expression several observations can be made. First, from the normalized transmission for a wafer with thickness d_1 , the normalized transmission of a wafer with thickness d_2 at the same temperature can easily be calculated, i.e.,

$$t(T, d_2) = t(T, d_1)^{(d_2/d_1)}. \quad (5)$$

Second, from measurements of normalized transmission, one can easily extract the absorption coefficient $\alpha(T)$, as-

suming the normalization temperature absorption coefficient is known.

$$\alpha(T) = \alpha(NT) - \frac{1}{d} \ln [t(T)]. \quad (6)$$

For most cases of interest, the absorption coefficient at the normalization temperature (typically room temperature) is negligible; this will be addressed in more detail later in the paper, however.

III. NEAR-INFRARED ABSORPTION PROCESSES IN SILICON

In earlier work [3], the absorption coefficients of lightly doped silicon from 500 to 800°C at 1.30 and 1.55 μm were measured by extracting them from normalized transmission. The fundamental absorption processes were not identified however. In this section, analytical expressions for various absorption processes are presented. In the next section, these models will be compared to data to determine the dominant processes.

Near-infrared absorption in silicon proceeds predominantly by two processes: valence band to conduction band transitions and by free carrier absorption. Because the band-to-band (bandgap) absorption is an indirect process which requires a phonon, and because the bandgap decreases as temperature increases, this process becomes stronger as temperature increases. Free carrier absorption also increases with temperature for two reasons. First, the scattering rate of the excited carriers increases with temperature, producing a larger absorption cross section for each carrier. Second, the carrier concentration will increase with temperature because of the larger intrinsic carrier concentration.

A first principles model of band-to-band absorption near the bandgap in silicon has been developed by Macfarlane *et al.* [7]. It was found that such absorption is due to phonon-assisted indirect transitions from the Γ_{25}' point in the valence band to a point along the Δ branch in the conduction band. The two dominant phonon energies are 212K and 670K, and were thought by Macfarlane *et al.* to be the transverse and longitudinal acoustic phonons with K vectors in the $\langle 100 \rangle$ direction. (It is now known however, that the 670K phonon which dominates absorption is the transverse-optical, not longitudinal-acoustic [8].) Phonons may be either absorbed or emitted in the optical absorption process. Macfarlane's model was refined by Jellison *et al.* [5] to give an expression for the bandgap absorption

$$\begin{aligned} \alpha_{BG}(h\nu, T) &= \sum_{i=1}^2 \sum_{l=1}^2 (-1)^l \frac{\alpha_i [h\nu - E_g(T) + (-1)^l k\theta_i]}{\exp [(-1)^l \theta_i / T] - 1} \text{ cm}^{-1} \end{aligned} \quad (7)$$

where $i = 1$ and 2 represent the transverse acoustic and optical phonon processes, respectively, and $l = 1$ and 2 represent phonon emission and absorption, respectively.

$h\nu$ is the photon energy, T is the temperature, k is Boltzmann's constant, and the θ_i are the phonon energies (transverse acoustic, 212K; transverse optical, 670K). The denominator arises from the Bose-Einstein phonon population. $\alpha_1(E)$ and $\alpha_2(E)$ represent absorption from the transverse acoustic and optical phonons, respectively.

$$\begin{aligned}\alpha_1(E) &= 0.504 \sqrt{E} + 392(E - 0.0055)^2, \\ &E \geq 0.0055 \\ &= 0.504 \sqrt{E}, \quad 0 \leq E \leq 0.0055 \\ &= 0, \quad E < 0\end{aligned}\quad (8)$$

$$\begin{aligned}\alpha_2(E) &= 18.08 \sqrt{E} + 5760(E - 0.0055)^2, \\ &E \geq 0.0055 \\ &= 18.08 \sqrt{E}, \quad 0 \leq E \leq 0.0055 \\ &= 0, \quad E < 0\end{aligned}\quad (9)$$

where α is in units of cm^{-1} and E is in electronvolts. The temperature dependence of the bandgap $E_g(T)$ is also well known.

$$E_g(T) = E_g^0 - \frac{AT^2}{B + T} \text{ eV} \quad (10)$$

where $A = 4.73 \times 10^{-4} \text{ eV/K}$ and $B = 635 \text{ K}$ [9]. Instead of the common $E_g^0 = 1.17 \text{ eV}$, we will follow the formulation of Jellison [5] and subtract an exciton energy of $\sim 15 \text{ meV}$ to get $E_g^0 = 1.155 \text{ eV}$. Using (7)–(10), the band-to-band optical absorption near the bandgap can now be calculated for arbitrary temperature and wavelength.

The second absorption mode is absorption by free carriers. From the plasma frequency, one can calculate the free-carrier absorption by first principles. This requires knowledge of the mobility and hot carrier scattering rates at high temperatures which are not known, however. The dependence of free-carrier absorption cross section on temperature has been measured at $1.06 \mu\text{m}$ from 100 to 400 K, and a linear dependence was found for the total free-carrier absorption cross section ($\sigma_n + \sigma_p$) [10]. We will extrapolate this linear dependence to the range of our work, up to 850°C , and later find this to be an excellent assumption. Measurements of free-carrier absorption at room temperature and a doping of 10^{18} cm^{-3} show the electron absorption to be twice as strong as the hole absorption ($\alpha = 8 \text{ cm}^{-1}$ versus 4 cm^{-1}) [11]. Dividing the cross sections of [10] into electron and hole contributions according to the above ratio, and also assuming a classical λ^2 wavelength dependence, one arrives at

$$\begin{aligned}\sigma_n(T) &= 1.01 \times 10^{-12} \cdot T \cdot \lambda^2 \text{ K}^{-1} \\ \sigma_p(T) &= 0.51 \times 10^{-12} \cdot T \cdot \lambda^2 \text{ K}^{-1}.\end{aligned}\quad (11)$$

The electron and hole concentrations n and p depend on doping and n_i according to the usual formulas. The intrinsic carrier concentration was calculated from

$$\begin{aligned}n_i &= 3.87 \times 10^{16} \cdot T^{3/2} \exp(-(0.605 + \Delta\epsilon)/kT) \\ \Delta\epsilon &= -7.1 \times 10^{-10} \sqrt{n_i/T}\end{aligned}\quad (12)$$

where T is in kelvins and n_i in cm^{-3} [9]. Knowing the carrier concentrations and absorption cross sections, the free carrier absorption coefficient can be calculated as

$$\alpha_{FC}(T) = n(T) \cdot \sigma_n(T) + p(T) \cdot \sigma_p(T). \quad (13)$$

The total absorption coefficient (used in (1)–(6), e.g.) is, of course, the sum of the free-carrier absorption $\alpha_{FC}(T)$ and the bandgap absorption $\alpha_{BG}(T)$. It should also be pointed out that while both mechanisms increase with temperature, they differ in their wavelength dependence. Band-to-band absorption should increase sharply with increasing photon energy, while free-carrier absorption should actually decrease with increasing photon energy ($\alpha \sim \lambda^2$).

More complicated physical effects, such as transitions to or from dopant energy levels, bandgap narrowing due to heavy doping, or absorption by phonon processes other than those described have been omitted for simplicity. This comes at the expense of some accuracy, but the model is sufficiently detailed to allow identification of the dominant processes as seen in the next section.

IV. DATA AND INTERPRETATION FOR LIGHTLY DOPED WAFERS

To make possible an accurate measurement of the true wafer temperature while measuring infrared transmission, all data presented in this paper were measured in a specially adapted conventional diffusion furnace. The temperature was measured by a thermocouple inserted into the furnace tube, with an estimated error of $\pm 5^\circ\text{C}$. The optical beam path was perpendicular to the length of the furnace tube through a small ($\sim 1 \text{ cm}$) hole cut in the heating coils and insulation surrounding the quartz tube. Error bars have been omitted on all data for clarity, but a conservative estimate of the error (due to drifts in the optical alignment at high temperature) is $\sim \pm 20\%$ of the measured signal. A normalization temperature of $30\text{--}35^\circ\text{C}$ was used in all cases. The difference in 30°C and a room-temperature normalization is negligibly small (estimated $< 1\%$ in all cases).

Shown in Fig. 2 are data for normalized transmission versus temperature for lightly doped p-type ($37 \Omega \cdot \text{cm}$, thickness = $493 \mu\text{m}$) and n-type ($7.5 \Omega \cdot \text{cm}$, thickness = $513 \mu\text{m}$) silicon $\langle 100 \rangle$ wafers. The actual data presented have been adjusted using (5) to reflect a $500\text{-}\mu\text{m}$ wafer for comparisons independent of wafer thickness. Note that within the experimental resolution, the data for the lightly doped n- and p-type wafers are identical. This is expected since for light dopings the wafers have negligible absorption at the normalization temperature ($\alpha \ll 1 \text{ cm}^{-1}$ based on [11] or (6)–(13)), and the wafers are "intrinsic" over the temperature range of interest ($n_i \approx 6 \times 10^{16} \text{ cm}^{-3}$ at 500°C). Also plotted in Fig. 2 are the results of the model for normalized transmission for a lightly doped n-type wafer ($N_A = 10^{15} \text{ cm}^{-3}$) of thickness $500 \mu\text{m}$. The agreement between the model and data for normalized transmission is strikingly good, especially

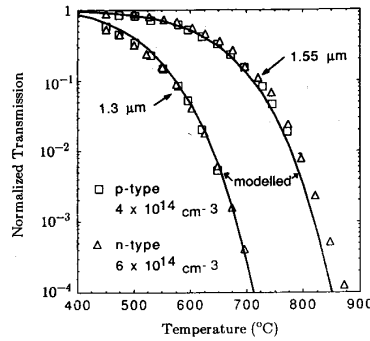


Fig. 2. Data of normalized transmission versus temperature for 1.30 and 1.55 μm , for lightly doped $\langle 100 \rangle$ n-type ($7.5 \Omega \cdot \text{cm}$, thickness = $513 \mu\text{m}$) and p-type ($37 \Omega \cdot \text{cm}$, thickness = $493 \mu\text{m}$). The data have been adjusted to reflect a $500\text{-}\mu\text{m}$ thickness. Also presented are the model results for the n-type wafer.

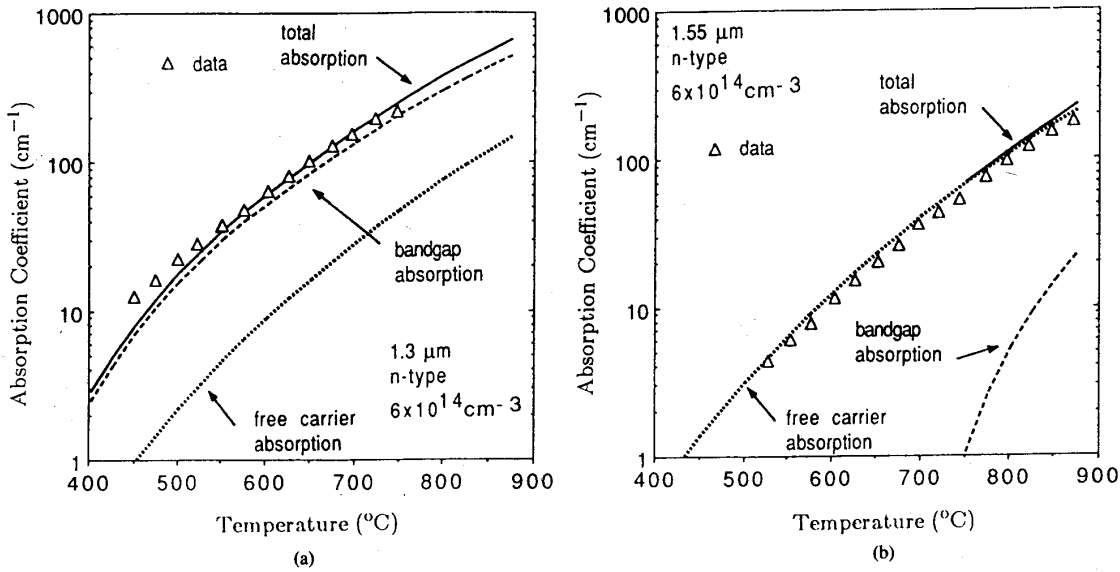


Fig. 3. Absorption coefficient versus temperature at (a) $1.30 \mu\text{m}$, and (b) $1.55 \mu\text{m}$, extracted from the n-type data of Fig. 2, along with modeled free-carrier, bandgap, and total absorption.

considering that no adjustable parameters were used in constructing the model.

In Fig. 3, the model components of free-carrier and interband absorption are plotted independently along with the total in comparison with data for lightly doped n-type wafers. One sees that absorption at both 1.30 and $1.55 \mu\text{m}$ are well approximated by the models. Nearly all of the absorption at $1.30 \mu\text{m}$ proceeds by a band-to-band process, while at $1.55 \mu\text{m}$ free-carrier absorption is predicted to be much stronger than band-to-band absorption. The good agreement at $1.55 \mu\text{m}$ indicates that the extrapolation of the free-carrier absorption cross sections of [10] to high temperatures described earlier is indeed a good approximation. To confirm the different mechanisms at 1.3 and $1.55 \mu\text{m}$, measurements on a lightly doped p-type wafer were repeated with the wavelength of each laser slightly shifted by "temperature tuning" the lasers. (1.30

μm , $\Delta\lambda \approx +10 \text{ nm}$, $1.55 \mu\text{m}$, $\Delta\lambda = +7 \text{ nm}$), and the new absorption coefficients were extracted (Fig. 4). Near $1.30 \mu\text{m}$, a clear decrease in absorption was evident at longer wavelengths, as expected for band-to-band absorption. At $1.55 \mu\text{m}$, a much smaller change in absorption, if any, of opposite sign from that at $1.30 \mu\text{m}$ was observed. This is consistent with the dominance of free-carrier absorption over band-to-band absorption, and the weaker energy dependence of free-carrier absorption, both in agreement with the model results. (Because the data of Fig. 4 were measured in a furnace without a calibrated thermocouple, they do not agree precisely with those of Fig. 3. All other data reported in this paper were taken from a single furnace with the thermocouple calibrated within the limits stated earlier.)

The dominant bandgap absorption at $1.3 \mu\text{m}$ implies that bandgap absorption also dominates at shorter wave-

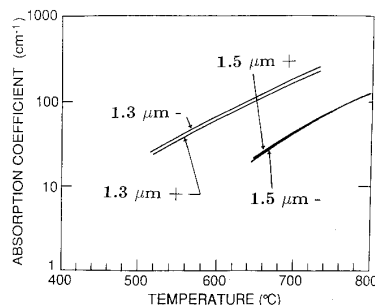


Fig. 4. Extracted absorption coefficients versus temperature for the p-type wafer of Fig. 2 for slight shifts in wavelength near 1.30 and 1.55 μm . The subscripts + and - refer to longer and shorter wavelengths, respectively, with the difference being ~ 10 nm for 1.30 μm and 8 nm for 1.55 μm .

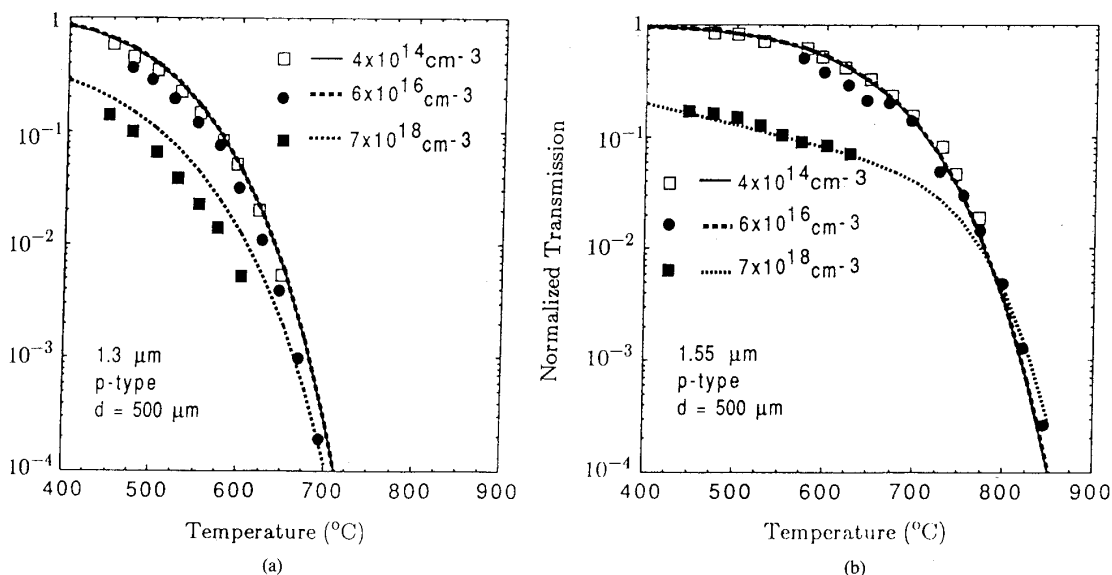


Fig. 5. Data (points) and simulation (lines) of normalized transmission versus temperature for various p-type doping levels for (a) 1.30 μm and (b) 1.55 μm . The data have been adjusted to represent 500- μm wafers.

lengths. This is consistent with previous results at 1.15 μm [5] where the absorption up to $\sim 840^\circ\text{C}$ was accurately modeled using only the bandgap absorption processes (7)–(10). Our results also imply a minimum in the absorption (maximum transmission) at elevated temperatures between 1.3 and 1.55 μm , which in turn implies a minimum in the emissivity. Such a minimum has indeed been observed in this wavelength range by Sato [1].

V. EFFECTS OF SUBSTRATE DOPING

Many semiconductor manufacturing applications require the use of substrates with moderate (10^{16} – 10^{17} cm^{-3}) or heavy ($> 10^{18}$ cm^{-3}) doping. In this section the effect of substrate doping on normalized transmission versus temperature is investigated. Physically, the heavily doped case is expected to be different than the lightly doped case because of the significant free-carrier absorption at room temperature. Other physical effects include the differing carrier concentration versus temperature relationships,

bandgap reduction at extremely high doping levels (increasing bandgap absorption), and significant occupation of band states (reducing band-to-band absorption). One might expect, that because of the normalization procedure, the extra free-carrier absorption from heavy doping would have little effect on the normalized transmission versus temperature. However, this is not true primarily because the extra absorption caused by the free carriers has approximately a linear temperature dependence. For example, if the substrate doping at 300 K has an absorption which reduces the transmission through the wafer by a factor of 3, at 900 K the free carriers would cause the transmission to drop by a factor of $3^{900/300} = 27$, a factor of 9 lower than the normalization value of 300 K.

Measurements of normalized transmission (normalization temperature = 30–35 $^\circ\text{C}$) on p-type $\langle 100 \rangle$ wafers with doping levels from 4×10^{14} to 7×10^{18} cm^{-3} are shown in Fig. 5 as points. To facilitate a visual interpretation of the data, all data in Fig. 5 were adjusted accord-

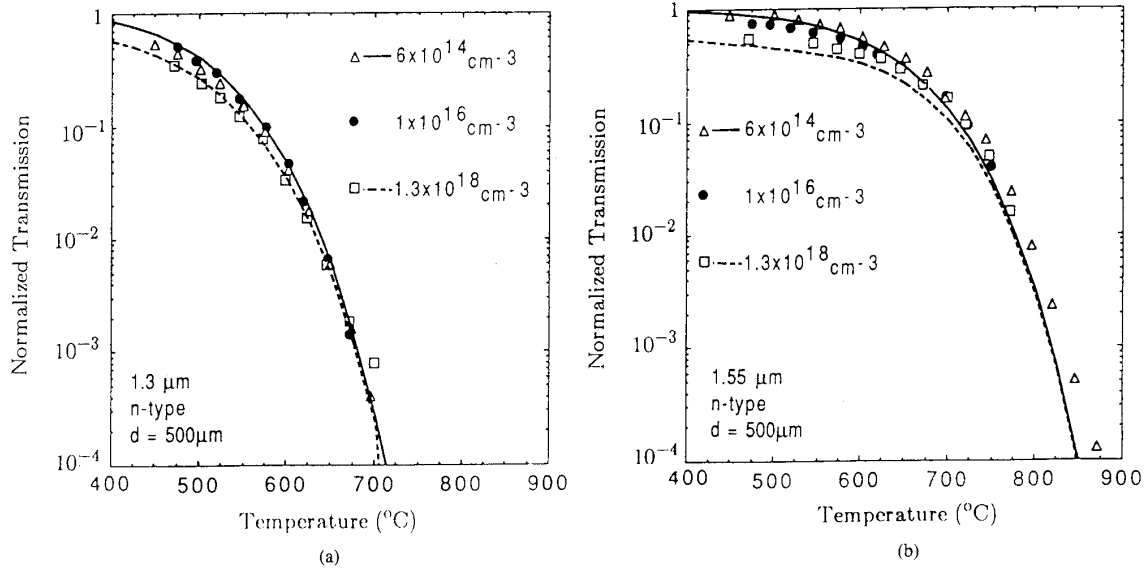


Fig. 6. Data and modeling of transmission for various dopings in n-type wafers for (a) 1.30 μm and (b) 1.55 μm . The data have been adjusted to represent 500- μm wafers.

ing to (5) to represent a wafer of 500- μm thickness; the actual wafers used had wafer thicknesses from 353 to 503 μm . The wafer with a doping level of $4 \times 10^{16} \text{ cm}^{-3}$ had a normalized transmission within the experimental error of that of the lightly doped wafer. A heavily doped p-type ($N_A = 7 \times 10^{18} \text{ cm}^{-3}$) did have a very low normalized transmission, due to the temperature dependence of the free-carrier absorption at room temperature as described above.

Simulation results of normalized transmission for the same dopings are also presented in Fig. 5. No parameters were adjusted, and again excellent agreement is seen between the simulation and experimental data. The modeling confirms that there should be no difference in the normalized transmission of lightly or moderately doped wafers, and that order of magnitude effects require a doping level in the 10^{19} cm^{-3} range. At high temperatures, even heavily doped samples should become intrinsic ($n_i = 10^{18} \text{ cm}^{-3}$ at $\sim 700^\circ\text{C}$). As would be expected, the differences in normalized transmission thus become smaller at higher temperature. Similar results presented in Fig. 6, are obtained for various n-type dopings (6×10^{14} , 1×10^{16} , $1.3 \times 10^{18} \text{ cm}^{-3}$). No adjustment of any parameters or incorporation of more complicated physical effects into the model (such as bandgap narrowing due to doping, degeneracy, etc.) was performed to obtain better quantitative agreement between the data and the model.

Simulations show that a doping level of $7 \times 10^{17} \text{ cm}^{-3}$ can be tolerated before a worst case deviation of 10% in the normalized transmission occurs for 500- μm wafers. Therefore, if one is satisfied with a 10% error in normalized transmission, one can use the infrared transmission technique to measure temperature using the temperature versus transmission curve for lightly doped wafers to infer temperature. Over the regions of the curve where we usu-

ally apply the technique in practice, a 10% error in transmission corresponds to a $\sim 3^\circ\text{C}$ error in temperature.

Absorption coefficients at elevated temperatures for the various doping levels were also extracted from the data of Figs. 5 and 6 using (6). This required a knowledge of the absorption coefficient at the normalization temperature ($\sim 35^\circ\text{C}$), which for heavy doping was obtained from the data of Soref *et al.* [10]. The data are presented in Fig. 7. This is the first time such data have been presented to the best knowledge of the authors.

VI. DISCUSSION

From knowledge of the absorption processes, one may draw some conclusions about the extension of the infrared transmission technique for measuring temperature to other wavelength/temperature ranges. For example, using a wavelength of 1.30 or 1.55 μm , the method is not practical for measurement below 500°C because of the weak dependence of transmission (and hence absorption constant) on temperature. However, since the dominant absorption at 1.30 μm is bandgap absorption, shorter wavelengths will give higher absorption coefficients and hence higher sensitivity at low temperature. For example, the absorption coefficient of silicon at 1.15 μm [5] and 1.054 μm [12] have been measured at elevated temperatures [5]. The results are similar to those in Fig. 2 at 1.30 μm , except shifted to lower temperatures by ~ 200 and 400°C , respectively. Therefore, the extension of the technique to temperatures at least as low as $\sim 100^\circ\text{C}$ (while maintaining high sensitivity) should be straightforward.

Our current upper temperature limit is $\sim 800^\circ\text{C}$, due to the weak 1.55- μm signal received. Higher temperatures will require wavelengths with less absorption. Since free-carrier absorption dominates in this range, longer wave-

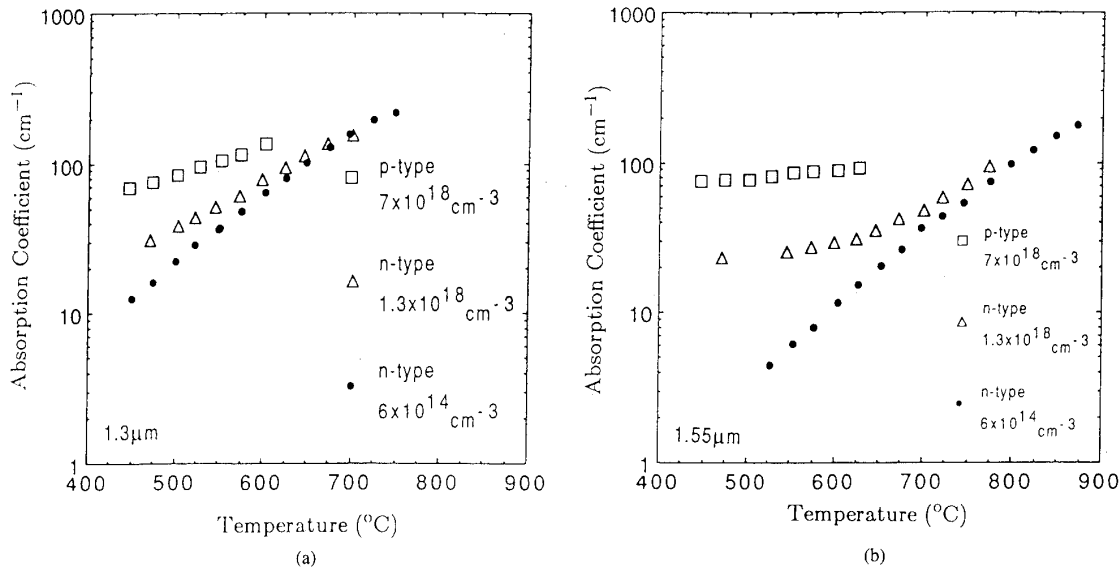


Fig. 7. Absorption coefficient of silicon at 1.30 and 1.55 μm at elevated temperatures for heavy doping for (a) 1.30 μm and (b) 1.55 μm .

lengths will have higher absorption than that at 1.55 μm . Slightly lower wavelengths should have somewhat less absorption, but by 1.30 μm the absorption is already an order-of-magnitude higher due to bandgap absorption. Indeed, a model calculation of the absorption coefficient from 600 to 800°C versus wavelength shows a minimum near 1.5 μm (Fig. 8). Therefore, it appears that it will be difficult to extend the infrared transmission technique to temperatures much higher than 800°C.

The use of (1)–(4) to measure temperature implicitly assume that the reflectivity $R(T)$ and the wafer thickness d are not changing as a function of time. In the case of silicon homoepitaxial growth, the reflectivity is constant but the wafer thickness is increasing. Using (5) one can easily calculate the effect of a change in wafer thickness on normalized transmission. For a nominal wafer thickness of 450 μm , a 5- μm increase in wafer thickness has been calculated to lead to only a 1°C error in the inferred temperature (assuming one did not correct for the increase in thickness). This is probably acceptable for most applications. The change in wafer thickness due to thermal expansion is $\sim 1 \mu\text{m}$ up to 800°C, and hence insignificant.

Field oxides will change the surface reflectivity R and emissivity, and can lead to pyrometry errors as large as 100°C if uncorrected [2]. Since the index of refraction for silicon dioxide is a weak function of temperature (as is that of silicon), changes in the transmission due to the different R for oxide-covered or patterned wafers should be removed by the normalization technique. To test this hypothesis, normalized transmission measurements were made on wafers with 2400 Å of oxide on the top side of a moderately doped n-type wafer, which should reduce the reflectivity at 1.3–1.5 μm from the usual $\sim 30\%$ to $\sim 5\%$. The wafers with oxide indeed had a normalized

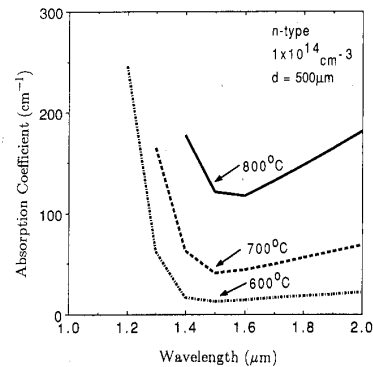


Fig. 8. Calculated absorption coefficients at 600, 700, and 800°C versus wavelength for lightly doped silicon.

transmission versus temperature indistinguishable within experimental error from that of the original substrate.

In the case the wafer surfaces were initially amorphous (from ion implantation, e.g.), the reflectivity would change as a function of time as the implants were annealed. Assuming that the entire probed surface consisted of this material (no masking oxide, etc.), that the infrared reflectivity upon annealing changes from ~ 0.4 to ~ 0.3 as in the visible, and a typical slope of 3%/°C in the normalized transmission (as in Fig. 2), this would cause about a 6°C error in the measured temperature.

VII. SUMMARY

The fundamental infrared absorption processes in silicon have been investigated at elevated temperatures. Because of the dominant bandgap absorption at 1.30 μm and

below, the prospects for extending the infrared transmission technique for RTP temperature measurement to temperatures as low as 100°C by using shorter wavelengths appear very good. Because of dominant free-carrier absorption at wavelengths over 1.55 μm , extending the technique above 800°C appears difficult, however. The normalized transmission versus temperature curves are similar for lightly doped n-type and p-type $\langle 100 \rangle$ wafers and little affected by substrate doping up to substrate doping levels of $\sim 10^{18} \text{ cm}^{-3}$, with significant changes at higher levels from free-carrier absorption. Finally, surface layers such as field oxides have little effect on the technique.

ACKNOWLEDGMENT

The assistance of P. V. Schwartz, M. Nardin, and K. Goel in the laboratory is appreciated.

REFERENCES

- [1] T. Sato, *Japan. J. Appl. Phys.*, vol. 6, pp. 339-347, 1967.
- [2] D. W. Pettibone, J. R. Suarez, and A. Gat, "The effect of thin dielectric films on the accuracy of pyrometric temperature measurement," in *Proc. Symp. Mat. Res. Soc.*, vol. 52, 1986, pp. 209-216.
- [3] J. C. Sturm, P. V. Schwartz, and P. M. Garone, "Silicon temperature measurement by infrared transmission for rapid thermal processing applications," *Appl. Phys. Lett.*, vol. 56, pp. 961-963, 1990.
- [4] J. C. Sturm and P. M. Garone, "Temperature control of silicon-germanium epitaxial growth on silicon substrates by infrared transmission," *J. Appl. Phys.*, vol. 69, pp. 542-544, 1991.
- [5] G. E. Jellison and D. H. Lowndes, "Optical absorption coefficient of silicon at 1.152 μ at elevated temperatures," *Appl. Phys. Lett.*, vol. 41, pp. 594-596, 1982.
- [6] F. Lukes, *J. Phys. Chem. Solids*, vol. 11, pp. 342-344, 1959.
- [7] G. G. Macfarlane, T. P. McLean, J. E. Quarrington, and V. Roberts, "Fine structure in the absorption-edge spectrum of Si," *Phys. Rev.*, vol. 111, pp. 1245-1254, 1958.
- [8] B. N. Brockhouse, "Lattice vibrations in silicon and germanium," *Phys. Rev. Lett.*, vol. 2, pp. 256-258, 1959.
- [9] C. D. Thurmond, "The standard thermodynamic functions for the formation of electrons and holes in Ge, Si, GaAs, and GaP," *J. Electrochem. Soc.*, vol. 122, pp. 1133-1141, 1975.
- [10] K. G. Svantesson and N. G. Nilsson, "Determination of the temperature dependence of the free carrier and interband absorption in silicon at 1.06 μm ," *J. Phys. C*, vol. 12, pp. 3837-3840, 1979.
- [11] R. A. Soref and B. R. Bennett, "Electrooptical effects in silicon," *IEEE J. Quantum Electron.*, vol. QE-23, pp. 123-129, 1987.
- [12] H. A. Weakliem and D. Redfield, *J. Appl. Phys.*, vol. 50, pp. 1491-1453, 1979.

*

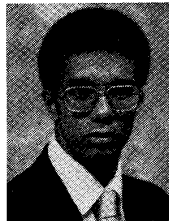


James C. Sturm (M'80-S'81-M'85) was born in Berkeley Heights, NJ, in 1957. He received the B.S.E. degree in electrical engineering and engineering physics from Princeton University, Princeton, NJ, in 1979, and the M.S.E.E. as well as Ph.D. degrees in 1981 and 1985, respectively, both from Stanford University, Stanford, CA. His Ph.D. dissertation investigated electronic devices and material properties for three-dimensional integration.

In 1979 he joined Intel Corporation as a microprocessor design engineer for one year. In 1981 he was a visiting scientist at Siemens Co., Munich, Germany. In 1986 he joined the faculty of Princeton University as an Assistant Professor in the Department of Electrical Engineering. He has worked in the fields of laser processing of semiconductors, thin epitaxial films, silicon-on-insulator, and three-dimensional integration. His current research interests include silicon-based heterojunctions, silicon-germanium growth and applications, silicon-based optoelectronics, and rapid thermal chemical vapor deposition.

Dr. Sturm is a member of the American Physical Society and the Materials Research Society, and is a National Science Foundation Presidential Young Investigator. He has served on the organizing committee of IEDM (1988-1989), on the IEDM Solid State Devices Subcommittee (1990-1991), as a symposium leader for the Materials Research Society (1987), and on the SOS/SOI Conference committee.

*



Casper M. Reeves (S'90) was born on April 2, 1969 and grew up in Cranford, NJ. He received the B.S. degree from Princeton University, Princeton, NJ in 1991, majoring in electrical engineering and engineering physics.

While at Princeton he examined several issues relevant to the growth of silicon-germanium epitaxial layers, including dislocation kinetics, optical and electrical properties, and temperature measurement. He is currently pursuing graduate study in electronic materials at the University of California at Santa Barbara.